Ultrasonics Sonochemistry 95 (2023) 106357

Contents lists available at ScienceDirect

Ultrasonics Sonochemistry

journal homepage: www.elsevier.com/locate/ultson

Sonoluminescence intensity and ultrasonic cavitation temperature in organic solvents: Effects of generated radicals

Ben Nanzai [a,*], Akimitsu Mochizuki [a], Yusuke Wakikawa [a], Yusuke Masuda [a], Tadashi Oshio [b], Kazuhiro Yagishita [b]

[a] Department of Materials and Life Science, Faculty of Science and Technology, Shizuoka Institute of Science and Technology, 2200-2 Toyosawa, Fukuroi, Shizuoka 437-8555, Japan

[b] Lubricants R&D Department, Lubricants Company, ENEOS Corporation, 8 Chidoricho, Naka-ku, Yokohama 231-0815, Japan

ARTICLE INFO

Keywords:
Methyl radicals
Methyl radial recombination method
Electron spin resonance
Vapor pressure
Viscosity
Surface tension

ABSTRACT

Ultrasonic cavitation in organic solvents remains poorly understood in contrast with aqueous systems, largely because of complexities related to solvent decomposition. In this study, we sonicated different types of organic solvents (i.e. linear alkanes, aliphatic alcohols, aromatic alcohols, and acetate esters) under argon saturation. The average temperature of the cavitation bubbles was estimated using the methyl radical recombination method. We also discuss the effects of the physical properties of the solvents, such as vapor pressure and viscosity, on the cavitation temperature. The average cavitation bubble temperature and sonoluminescence intensity were higher in organic solvents with lower vapor pressure; for aromatic alcohols, these values were particularly high. It was found that the specific high sonoluminescence intensities and average cavitation temperatures exhibited in aromatic alcohols are caused by the highly resonance-stable generated radicals. The results obtained in this study are very useful for acceleration of sonochemical reaction in organic solvents, which are indispensable for organic synthesis and material synthesis.

1. Introduction

The bubbles called ultrasonic cavitation may be generated by high-power ultrasonic irradiation into the liquid. The bubbles reach a critical size over a few acoustic cycles. These bubbles undergo quasi-adiabatic compression and develop into a reaction field with a high temperature (several thousand degrees) and pressure (several hundred atmospheres) [1,2]. The previous studies on the acoustic cavitation have mostly focused on aqueous solutions, and have mostly been conducted from the viewpoint of wastewater treatment. In aqueous solutions, reactive OH radicals and H radicals are formed by the sonolysis of water [3,4]. Therefore, it is considered that sonochemical degradation of organic compounds proceeds by pyrolysis inside cavities and by OH radicals in the interfacial region of the cavities. These radical species recombine to form water, hydrogen peroxide, or hydrogen. By contrast, there have been few reports in organic solvents [5,6]. This is because the pyrolysis products of solvent molecules are diverse, and they tend to lower the temperature of the cavitation bubbles [7–9]. Nevertheless, understanding the cavitation bubbles in organic solvents is important for organic synthesis, material synthesis, and the sonolysis of lipophilic compounds.

Most previous studies of sonochemistry organic solvents have been in the context of synthetic organic chemistry [10–12]. However, a study by Suslick et al. estimated the number and temperature of cavitation bubbles through ultrasonic irradiation of metal carbonyls in organic solvents [13]. Another study discussed the effect of solvent properties on reaction efficiency, but the discussion only considered the sonolysis product as a factor in complicating the sonochemical reaction, and did not provide sufficient clarification of the effects of these properties [5].

Several methods for evaluating the temperatures inside cavitation bubbles have been reported [13,19–21]. The most common method for estimating the peak temperature is based on the sonoluminescence intensity. Sonoluminescence is a phenomenon caused by the high temperatures and pressures inside cavitation bubbles [14]. Compression of bubbles occurs in a very short time (i.e. several nanoseconds) and the ensuing sonoluminescence pulse has duration of several tens to hundreds of picoseconds [15]. Although there is still discussion about the mechanism of sonoluminescence, the plasma emission theory is the

* Corresponding author.
E-mail address: nanzai.ben@sist.ac.jp (B. Nanzai).

https://doi.org/10.1016/j.ultsonch.2023.106357
Received 18 January 2023; Received in revised form 24 February 2023; Accepted 3 March 2023
Available online 7 March 2023

leading theory [16–18]. The glow of the bubble plasma consists of broadband spectrum similar to the blackbody radiation spectrum and (or) a white continuum of bremsstrahlung. These glows increase with the peak temperature, however, neither of these are luminescence. On the other hand, in the presence of luminophores or atoms, ions, radicals and molecular fragments generated by the thermal decomposition of primary molecules with luminophoric properties, these emitter particles emit light due to collisional excitation in the plasma, which is true luminescence. Therefore, sonoluminescence intensity is generally treated as an index of bubble peak temperature.

To estimate the average bubble temperature, the methyl radical recombination (MRR) method is commonly used [1,22–25]. This method is based on determining the temperature dependence of the rate constants for reactions between methyl radicals. Ethane and ethylene are produced by the recombination of two methyl radicals, which are decomposition products of hydrocarbon compounds. Acetylene is produced predominantly from the dehydrogenation of ethylene. The ratio of the sum of the ethylene and acetylene yields to the ethane yield is equal to the ratio between the rate constants for the formation of ethylene and ethane, as shown in eq. (1).

$$\left(y_{C_2H_2} + y_{C_2H_4}\right) / y_{C_2H_6} = k_{C_2H_4} / k_{C_2H_6} \quad (1)$$

where y is the molar yield of each gas and k is the rate constant for each reaction. The rate constant k_{C2H4} (1.0×10^{16} exp (-134 kJ mol^{-1}/RT) dm^3 mol^{-1} s^{-1}) is only weakly dependent, but k_{C2H6} (2.4×10^{14} $T^{-0.4}$ dm^3 mol^{-1} s^{-1}) depends significantly on temperature. Therefore, a change in the ratio of the product yields indicates a change in the temperature at which the recombination reactions occur. Previous studies suggest that the MRR method gives only spatial and temporal average temperature values and involves a number of assumptions [22,23]. Ciawi et al. proposed the following conditions for the use of the MRR method [25]: Methyl radicals produced by thermal decomposition are the main intermediates that produce ethane and ethylene. Acetylene is produced primarily by thermal dehydrogenation of ethylene. No significant side reactions associated with these gas products occur. These gas products are not disproportionately produced or consumed even if side reactions occur.

In the present study, we discuss the effects of the solvent properties (i.e. solvent vapor pressure, viscosity, and surface tension) on the temperature in cavitation bubbles produced in different organic solvents. We evaluated sonoluminescence intensity reflecting the peak temperature, in addition to the average temperature by the MRR method We also used electron spin resonance (ESR) to explain the influence of the solvent properties on the bubble temperature in terms of the difference in radical species formed.

2. Experimental section

2.1. Materials

The following 30 solvents (96.0%–99.0% pure) were used without purification: linear alkanes with different carbon chain length (n = 6–16); aromatic hydrocarbons; linear aliphatic alcohols with different carbon chain length (n = 1–9); aromatic alcohols with different carbon chain length of the alkyl group (n = 0–3); acetate esters; unsaturated hydrocarbons; and branched alkanes. Hexane, octane, nonane, decane, dodecane, tetradecane, hexadecane, toluene, styrene, methanol, ethanol, 1-heptanol, 1-octanol, 1,4-butanediol, benzyl alcohol, 2-phenylethanol, propyl acetate, *iso* -butyl acetate, *tert* -butyl acetate, butyl acetate, pentyl acetate, octyl acetate, 1-octadecene, and squalene were supplied by Wako Pure Chemical Industries, Ltd. (Osaka, Japan). Butylbenzene, *tert*-butylbenzene, octylbenzene, 1-nonanol, and 3-phenyl-1-propanol were supplied by Tokyo Chemical Industry Co., Ltd. (Tokyo, Japan). Diluted ethane and ethylene (99.5% pure) and undiluted acetylene (0.1% in N_2) were used as standard gases for gas chromatography. These gases were supplied by GL sciences Inc. (Tokyo, Japan). For the spin-trapping agent, we used 5,5-dimethyl-1-pyrroline N-oxide (DMPO; > 97.0% pure), which was supplied by Tokyo Chemical Industry Co., Ltd. (Tokyo, Japan).

2.2. Estimation of the average cavitation bubble temperature

Ultrasonic irradiation was performed with a 78-kHz ultrasonic transducer (QUAVA mini QR-001; KAIJO, Tokyo, Japan), which was operated at 80 W. The diameter and base thickness of the reaction vessel were 55 and 1 mm, respectively. Each solvent (60 mL) was argon-saturated in the reaction vessel before being sonicated in an acrylic water bath, the temperature of which was maintained at 20 °C by a water circulation system with a temperature controller (4VT; Kyowa Interface Science Co. Ltd.). The yields of ethane, ethylene, and acetylene produced by sonication were quantified using gas chromatography with a flame ionization detector (GC-2025; Shimadzu Corp.) and an Alumina BOND/Na_2SO_4 column (RESTEK). Gas samples were taken from the headspace (130 mL) of the vessel for analysis after 30 min' sonication. The net yield of the decomposition products was obtained from the gas–liquid equilibrium constant in each solvent, and the average cavitation bubble temperature was estimated from the ratio of these yields.

2.3. Sonoluminescence measurements

Ultrasonic irradiation was performed with a 200-kHz ultrasonic transducer (QUAVA mini QR-003; KAIJO, Tokyo, Japan), which was operated at 100 W. The reaction vessel, gas atmosphere, and cooling system were the same as those described in the preceding section. A schematic diagram of this ultrasonic irradiation and sonoluminescence intensity measurement system is shown in Fig. 1. For sonoluminescence measurements, a blackout curtain was placed over the sonication bath. The light-receiving surface of the photomultiplier tube (PMT; H11890-110; Hamamatsu Photonics K.K.) was placed at the wall of the

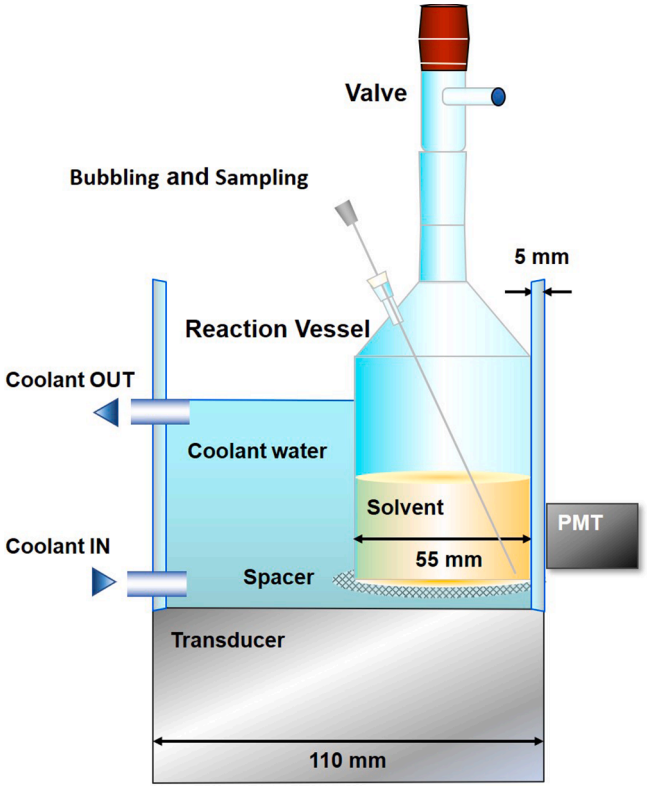

Fig. 1. Schematic diagram of ultrasonic irradiation and sonoluminescence intensity measurement system.

sonication bath (5 mm thick). The sensitivity wavelength range of this PMT is 230–700 nm. The sonoluminescence intensity obtained in this study is the value transmitted through the glass wall of reaction vessel and the acrylic wall of the irradiation bath. It was confirmed that the background sonoluminescence intensity in the absence of ultrasonic irradiation is sufficiently low at several to several tens of counts and can be ignored. Ultrasonic irradiation was started after 5 min of photon counting with the photomultiplier tube and was continued for 30 min.

2.4. ESR measurements

The sonication conditions, reaction vessel, atmosphere gas, and cooling system were the same as those used for sonoluminescence measurements. After argon bubbling, 60 μL of spin-trapping agent was added to the solvent. Sonication was then performed. The ESR spectra were recorded in a quartz aqueous cell at room temperature with X-band ESR spectrometer (RE1X, JEOL). ESR spectral simulation was performed in Matlab using the EasySpin package [26].

2.5. Measurement of physical properties

The viscosity of each solvent was measured using a viscometer (SV-10; A&D Co., Ltd.) at room temperature (25 °C). The surface tension of each solvent was measured using a contact angle meter (Drop Master DM-501; Kyowa Interface Science Co. Ltd.) at room temperature. Vapor pressure values were taken from the PubChem, chemical molecule database maintained by the National Center for Biotechnology Information (NCBI) [27].

3. Results and discussion

3.1. Physical properties of solvents

On the basis of previous reports, we considered the vapor pressure, viscosity, and surface tension values as the main physical properties of the solvent that affect the formation of bubbles (for example, by influence the cavitation threshold) and the growth and collapse of bubbles. The vapor pressure, viscosity, and surface tension of each solvent are presented in Table 1. The viscosities of hexane and octane were below the detection limit (0.30 mPa/s) and could not be measured. For most solvents (and for especially linear alkanes and aliphatic alcohols), a longer carbon chain length corresponded to a lower vapor pressure and higher viscosity. However, this trend did not apply to aromatic alcohols, for which the effect of carbon chain length was small. The surface tension also depended on the carbon chain length. In the next section, we investigate the relationship between the physical properties of each solvent and the average cavitation temperature.

3.2. Hydrocarbon products from sonochemical pyrolysis

The yields of ethane, ethylene, and acetylene generated from sonication for each solvent are shown in Fig. 2. These gases were not detectable from the solvent with high vapor pressure such as hexane, octane, toluene, styrene, methanol, ethanol, propyl acetate, *iso*-butyl acetate, and *tert*-butyl acetate. For all solvents, the yields decreased with increasing solvent vapor pressure. Especially for the linear alkanes and aliphatic alcohols, the yields of all gases increased with increasing solvent vapor pressure before reaching a maximum value, and a higher vapor pressure of the hydrocarbon gas correlated with a lower yield. *tert*-butylbenzene produced more ethane than the other aromatic hydrocarbons. We attribute this to the recombination of a large number of methyl radicals generated by the decomposition of the *tert*-butyl group [23]. 1-Octadecene generated more decomposition products than the other solvents, but no decomposition was observed with squalane, which has a similar vapor pressure. This is probably because the viscosity of squalane is more than eight times higher than that of 1-octadecene and the other solvents, which means that the sound pressure may not exceed the cavitation threshold under the conditions of our experiment [28]. For the aromatic alcohols, the yields of ethane and ethylene were lower than that of acetylene. Ciawi et al. reported that this tendency was observed in the ultrasonic decomposition of compounds that do not have a direct source of methyl radicals, such as aromatic compounds [29]. No decomposition product was observed in solvents with vapor pressure higher than that of octane (14.1 mmHg).

Based on these results, we make the following three inferences. (i) Solvents with extremely low vapor pressure do not decompose because the solvent vapor does not volatilize inside the cavitation bubble. (ii) As the vapor pressure increases, the amount of volatilization into the

Table 1
The vapor pressure (literature values taken from the PubChem [27]), viscosity, and surface tension (experimental values) of each solvent.

		Vapor pressure / mmHg	Viscosity / mPa s^{-1}	Surface tension / mN m^{-1}
linear alkanes	hexane	1.53×10^{2}		20.8
	octane	1.41×10^{1}		21.8
	nonane	4.45×10^{0}	0.50	23.2
	decane	1.43×10^{0}	0.65	24.1
	dodecane	1.35×10^{-1}	1.06	25.2
	tetradecane	1.50×10^{-2}	1.68	26.4
	hexadecane	1.43×10^{-3}	2.60	27.5
aliphatic alcohols	methanol	$1,27 \times 10^{2}$	0.43	10.5
	ethanol	$5,93 \times 10^{1}$	0.86	19.0
	1-heptanol	2.16×10^{-1}	5.41	27.3
	1-octanol	7.94×10^{-2}	7.13	28.5
	1-nonanol	2.27×10^{-2}	9.17	28.5
	1,4-butanediol	1.05×10^{-2}	67.98	45.2
aromatic alcohols	benzyl alcohol	9.40×10^{-2}	5.31	41.0
	2-phenylethanol	8.68×10^{-2}	10.79	42.9
	3-phenyl-1-propanol	2.34×10^{-2}	15.48	41.1
acetate esters	propyl acetate	3.59×10^{1}	0.44	24.7
	butyl acetate	1.15×10^{1}	0.55	25.2
	iso-butyl acetate	1.78×10^{1}	0.50	19.1
	tert-butyl acetate	4.70×10^{1}	0.51	19.0
	pentyl acetate	3.50×10^{0}	0.70	25.2
	octyl acetate	2.18×10^{-1}	1.41	26.9
aromatic hydrocarbons	toluene	2.84×10^{1}	0.44	29.4
	styrene	6.40×10^{0}	0.62	33.0
	butyl benzene	1.06×10^{0}	1.15	30.0
	tert-butyl benzene	2.20×10^{0}	0.86	29.3
	octyl benzene	1.12×10^{-2}	2.90	29.9
	diphenylmethane	8.21×10^{-3}	2.65	39.9
unsaturated hydrocarbon	1-octadecene	6.75×10^{-5}	3.38	29.5
branched hydrocarbon	squalane	6.30×10^{-6}	27.18	28.8

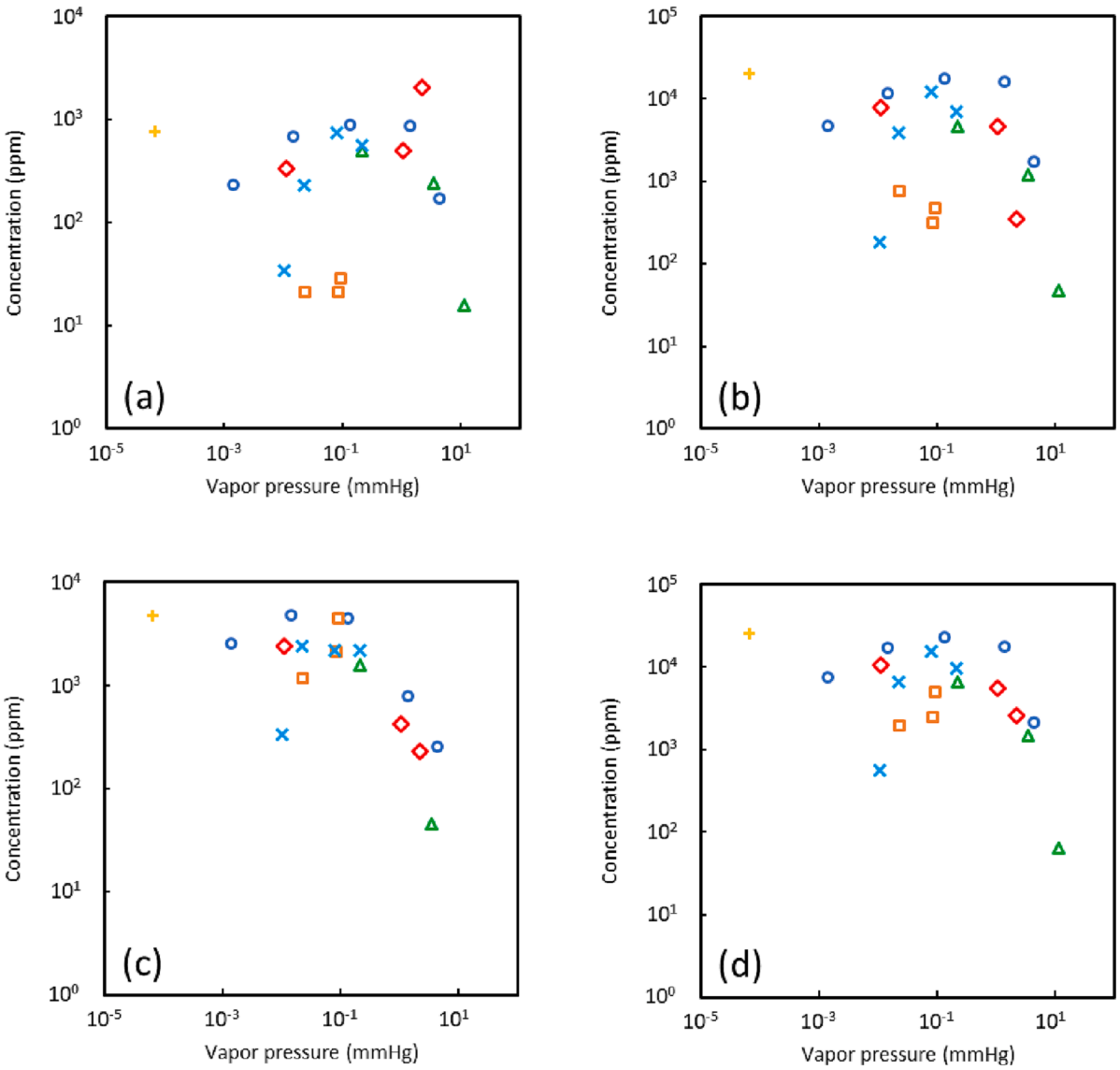

Fig. 2. Yields of (a) ethane, (b) ethylene, (c) acetylene and (d) their sum generated from the sonication for each solvent: linear alkanes (○), aromatic alcohols (□), acetate esters (△), aliphatic alcohols (×), aromatic hydrocarbons (◇), and unsaturated hydrocarbons (+).

bubble increases, resulting in an increase in the amount of decomposition products. (iii) Further increase in the solvent vapor pressure in the bubble reduces the specific heat ratio in the bubble and quenching sonoluminescence.

3.3. Average cavitation temperature

Fig. 3 shows the average temperature of the cavitation bubbles in each solvent estimated using the MRR method from the production ratio of ethane, ethylene, and acetylene by sonication for 30 min. The average cavitation temperature decreased with increasing solvent vapor pressure. The dependence of the cavitation temperature on the specific heat ratio is described by the Neppiras equation (Eq. (2) for quasi-adiabatic compression [30]:

$$T_{max} = \frac{P_{max}}{P}(\gamma - 1) \times T_0 \quad (2)$$

where T_{max} is the maximum bubble temperature, P_{max} is the maximum pressure when the bubble collapses, P is the sum of the atmospheric gas pressure and the solvent vapor pressure, γ is the specific heat ratio, and T_0 is the bulk temperature (20 °C). P_{max}, which depends on the output of the sonication device, was constant. The specific heat ratio, γ, of argon gas (1.67), which is a monatomic molecule, is higher than that of hydrocarbons, such as ethane (1.19), ethylene (1.24), acethylene (1.23), nonane (1.03), decane (1.03), and dodecane (1.02). At the start of sonication, the cavitation was filled with argon, resulting in a high specific heat ratio. During sonication, the solvent and decomposition products volatilized, thereby lowering the specific heat ratio and average temperature in the bubble. When the vapor pressure is extremely low, the solvent does not volatilize into the cavitation, so the obtained average temperature was assumed to be the cavity temperature without quenching. We estimated this to be approximately 4400 K, which is close to the values previously estimated from other methods [13,19–21]. For the aromatic alcohols, the estimated temperature was higher than for other solvent species. We discuss the reason for this in the next section.

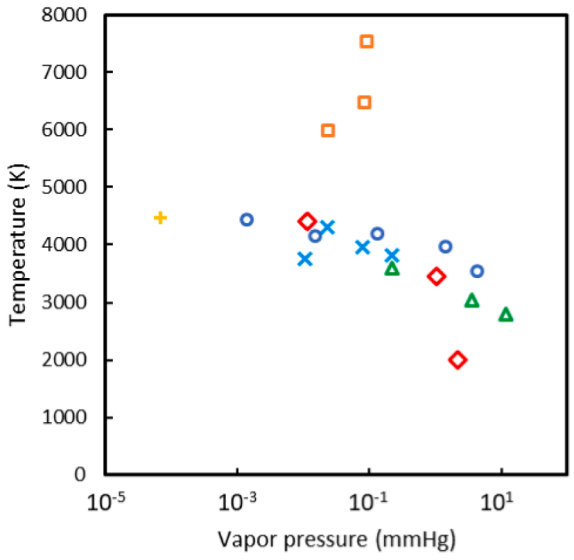

Fig. 3. Relationship between the solvent vapor pressure and average temperature in cavitation bubbles formed in each solvent: linear alkanes (○), aromatic alcohols (□), acetate esters (△), aliphatic alcohols (×), aromatic hydrocarbons (◇), and unsaturated hydrocarbons (+).

3.4. Sonoluminescence intensity

Fig. 4 shows the relationship between the vapor pressure and the average sonoluminescence intensity; the error bars indicate the maximum and minimum intensities over the 30-minute sonication period. The sonoluminescence intensity decreased with increasing vapor pressure. We attribute this to the bubble temperature being lowered by solvent evaporating into the bubble. Sonoluminescence was observed even above the threshold vapor pressure of 14.1 mmHg for sonolysis of solvents as described above section. Preliminary experiments have confirmed that this is luminescence from the cooling water around the reaction vessel, and solvents with vapor pressure higher than the threshold do not emit light. This result also indicates that sonoluminescence from the cooling water contributed to the observed signal in addition to that form the target solvent. Similar to the results of the average cavitation temperature described above, high sonoluminescence intensities were observed from aromatic alcohols, especially benzyl alcohol. We found that in aromatic alcohols, especially benzyl alcohol, the temperature was independent of the vapor pressure. A previous report showed that the sonoluminescence intensity depends on (surface tension)^2/vapor pressure [31]. Sonoluminescence intensity showed a better correlation with this value than only vapor pressure. This is a proposed value based on the influence of surface tension on the size of cavitation bubbles and their growth and collapse. However, the results for aromatic alcohols obtained in the present study do not fit this trend, as shown in Fig. 5. We found a positive correlation between the average cavitation temperature and the sonoluminescence intensity as shown in Fig. 6, suggesting that the high temperature of cavitation bubbles in benzyl alcohol is not an apparent value but an actual value. Thus, the limitations of the MRR method proposed by Ciawi et al. [29] do not apply to our study.

3.5. Effect of generated radicals

We suggest that differences in the radical species generated by sonolysis account for the cavitation bubble temperature among different organic solvents. Benzyl alcohol has no source of methyl radicals, and thereby the yield of ethane and ethylene generated by recombination of methyl radicals was low, as shown in Fig. 1. To confirm the absence of methyl radicals during sonication of benzyl alcohol, we conducted ESR measurements. As shown in Fig. 7, the simulation of the observed ESR spectrum indicates the presence of two radical species trapped in DMPO, which are attributed to the benzyl (A_N = 1.52 mT, A_H = 2.15 mT)

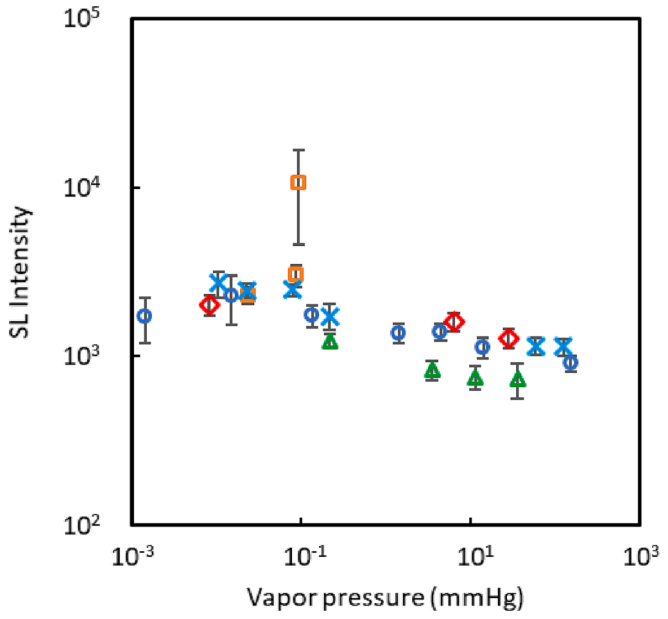

Fig. 4. Relationship between solvent vapor pressure and the sonoluminescence (SL) intensity. Error bars indicate the standard deviation of sonoluminescence intensities from 30 min of sonication for each solvent: linear alkanes (○), aromatic alcohols (□), acetate esters (△), aliphatic alcohols (×), and aromatic hydrocarbons (◇).

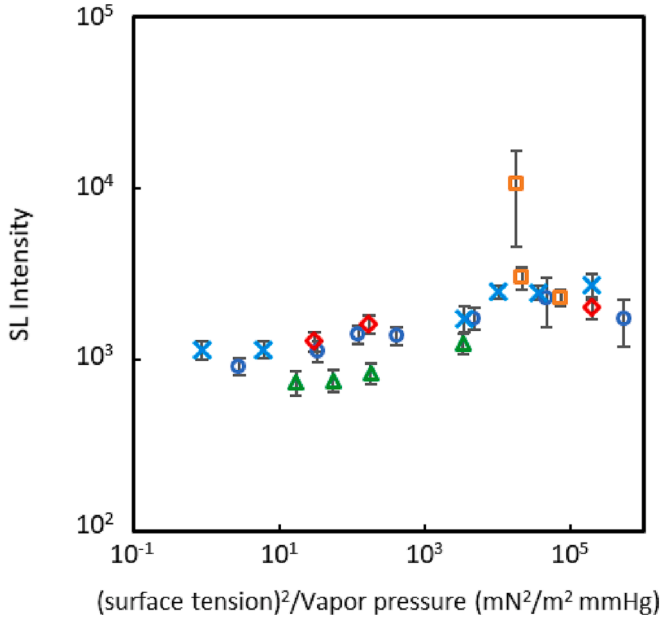

Fig. 5. Relationship between the value of (surface tension)^2/vapor pressure and sonoluminescence (SL) intensity. Error bars indicate the standard deviation of sonoluminescence intensities from 30 min of sonication for each solvent: linear alkanes (○), aromatic alcohols (□), acetate esters (△), aliphatic alcohols (×), and aromatic hydrocarbons (◇).

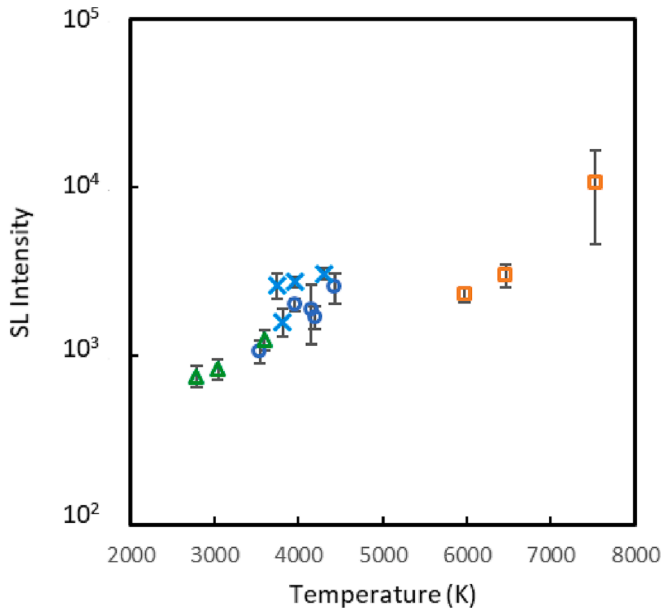

Fig. 6. Relationship between the average bubble temperature and the sonoluminescence (SL) intensity. Error bars indicate the standard deviation of sonoluminescence intensities from 30 min of sonication for each solvent: linear alkanes (○), aromatic alcohols (□), acetate esters (△), and aliphatic alcohols (×). Data for the aromatic hydrocarbons were not available.

[32–34] and OH ($A_N = 1.40$ mT, $A_H = 1.10$ mT) [34] radicals rather than methyl radical. In contrast with the methyl radical, the benzyl radical is resonantly stable and therefore does not recombine to generate products that lower the bubble temperature and quench sonoluminescence. Therefore, the cavitation bubbles formed in benzyl alcohol retained a high average temperature relative to the vapor pressure. The high temperature of cavitation bubbles in benzyl alcohol favors the formation of acetylene, which requires the cleavage of the C = C bond of the stable benzene ring and the formation of CH radicals [29]. The high sonoluminescence intensity from aromatic alcohols can also be explained by the high bubble temperature. These conditions favor the generation of OH radicals, which may also contribute to the sonoluminescence intensity [35]. The higher sonoluminescence intensity from aliphatic alcohols than from other solvents, such as alkanes and esters, also supports this inference. We also measured the sonoluminescence intensity for a system using phenol as a solvent, and found that the intensity was about 700, which is much lower than that of other aromatic alcohols that produce benzyl radicals. To confirm whether the bubble temperature in the aromatic alcohols was higher than in the other solvents, as a preliminary study, we observed the ultrasonic decomposition of the fluorosurfactant perfluorodecanoic acid, which is an extremely persistent compound, using 1-octanol and benzyl alcohol as solvents. The vapor pressures of 1-octanol and benzyl alcohol are almost the same (7.94×10^{-2} and 9.40×10^{-2} mmHg, respectively). The cavitation average temperature obtained in this study was about two times higher for benzyl alcohol than for 1-octanol. As a result, almost no degradation of this fluorosurfactant was observed in 1-octanol, whereas a significant decrease in concentration was observed in benzyl alcohol. This confirmed the high temperature of the cavitation bubbles formed in benzyl alcohol. The results of present study indicate that not only the physical properties, such as vapor pressure and surface tension of the solvent, but also structural factors such as resonance stability contribute to the high cavitation bubble temperature.

4. Conclusions

For cavitation in different organic solvents, we estimated the peak bubble temperature from the sonoluminescence intensity and the average temperature using the MRR method. We found that the solvent vapor pressure influences the cavitation temperature, in addition, radical species generated by the sonochemical pyrolysis of the solvent have a great effect on the cavitation temperature. The product of methyl radical recombination lowers the cavitation temperature, while the resonance-stable benzyl radical is less likely to recombine and the cavitation temperature remains high. Our results may allow for the design of sustainable high-temperature reaction fields that drive ultrasonic chemical reactions more effectively for organic synthesis and material synthesis in the future.

Author contribution statement

BN supervised the conduct of this study and drafted the original manuscript. AM and YM performed ultrasonic irradiation, sonoluminescence measurement, and physical property measurement. YW carried out ESR analysis and radical species identification. TO and KY

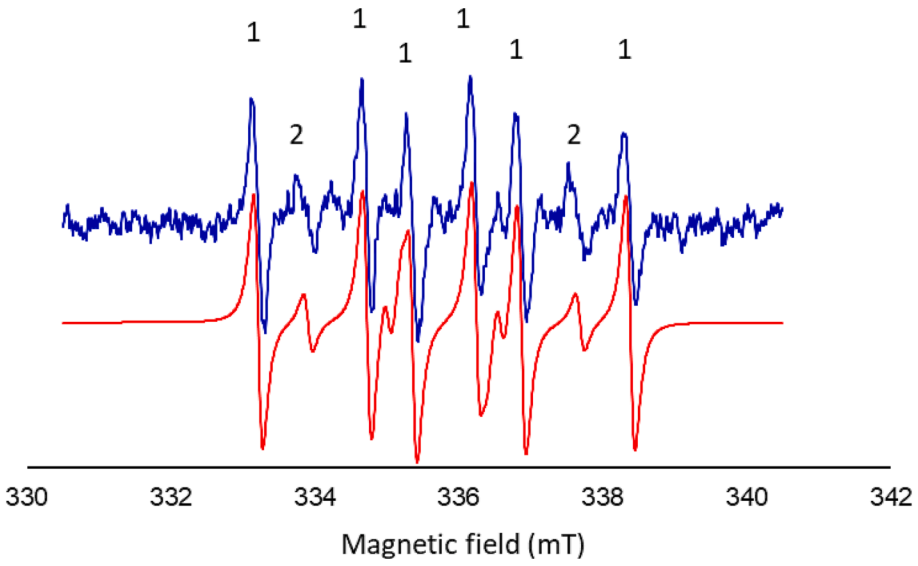

Fig. 7. Electron spin resonance spectrum and a simulated spectrum following sonication at 200 kHz of benzylalcohol in the presence of DMPO (10 mM). The lines in the spectrum represent benzyl ('1') and OH radicals ('2').

contributed to the interpretation of the results. All authors reviewed the manuscript draft and revised it critically on intellectual content. All authors approved the final version of the manuscript to be published.

Declaration of Competing Interest

The authors declare that they have no known competing financial interests or personal relationships that could have appeared to influence the work reported in this paper.

Acknowledgments

The authors are grateful to Mr. Kazuya Hikida and Ms. Miyu Murayama for assistance. We thank Adam Brotchie, PhD, from Edanz (https://jp.edanz.com/ac) for editing a draft of this manuscript. This work was supported by JSPS KAKENHI (Grant Number 19 K05572 / 22 K05199).

References

[1] K. Okitsu, T. Suzuki, N. Takenaka, H. Bandow, R. Nishimura, Y. Maeda, Acoustic multibubble cavitation in water: a new aspect of the effect of a rare gas atmosphere on bubble temperature and its relevance to sonochemistry, J. Phys. Chem. B 110 (2006) 20081–20084, https://doi.org/10.1021/jp064598u.
[2] W.B. McNamara III, Y.T. Didenko, K.S. Suslick, Pressure During Sonoluminescence, J. Phys. Chem. B 107 (2003) 7303–7306, https://doi.org/10.1021/jp034236b.
[3] A.E. Alegria, Y. Lion, T. Kondo, P. Riesz, Sonolysis of aqueous surfactant solutions: probing the interfacial region of cavitation bubbles by spin trapping, J. Phys. Chem. 93 (12) (1989) 4908–4913, https://doi.org/10.1021/j100349a046.
[4] C.M. Krishna, T. Kondo, P. Riesz, Sonochemistry of alcohol–water mixtures: spin-trapping evidence for thermal decomposition and isotope-exchange reactions, J. Phys. Chem. 93 (1989) 5166–5172, https://doi.org/10.1021/j100350a029.
[5] Y. Mizukoshi, H. Nakamura, H. Bandow, Y. Maeda, Y. Nagata, Sonolysis of organic liquid: effect of vapour pressure and evaporation rate, Ultrason. Sonochem. 6 (1999) 203–209, https://doi.org/10.1016/S1350-4177(99)00012-7.
[6] K.S. Suslick, J.J. Gawienowski, P.F. Schubert, H.H. Wang, Sonochemistry in non-aqueous liquids, Ultrason. 22 (1984) 33–36, https://doi.org/10.1016/0041-624X(84)90059-3.
[7] M. Ashokkumar, R. Hall, P. Mulvaney, F. Grieser, Sonoluminescence from Aqueous Alcohol and Surfactant Solutions, J. Phys. Chem. B 101 (1997) 10845–10850, https://doi.org/10.1021/jp972477b.
[8] M. Ashokkumar, P. Mulvaney, F. Grieser, The effect of pH on multibubble sonoluminescence from aqueous solutions containing simple organic weak acids and bases, J. Am. Chem. Soc. 121 (1999) 7355–7359, https://doi.org/10.1021/ja990482i.
[9] G.J. Price, M. Ashokkumar, F. Grieser, Sonoluminescence quenching of organic compounds in aqueous solution: frequency effects and implications for sonochemistry, J. Am. Chem. Soc. 126 (2004) 2755–2762, https://doi.org/10.1021/ja0389624.
[10] T.J. Mason, Ultrasound in synthetic organic chemistry, Chem. Soc. Rev. 26 (1997) 443–451, https://doi.org/10.1039/CS9972600443.
[11] B. Banerjee, Recent developments on ultrasound assisted catalyst-free organic synthesis, Ultrason. Sonochem. 35 (2017) 1–14, https://doi.org/10.1016/j.ultsonch.2016.09.023.
[12] I.V. Machado, J.R.N. dos Santos, M.A.P. Januario, A.G. Corrêa, Greener organic synthetic methods: Sonochemistry and heterogeneous catalysis promoted multicomponent reactions, Ultrason. Sonochem. 78 (2021), 105704, https://doi.org/10.1016/j.ultsonch.2021.105704.
[13] K.S. Suslick, D.A. Hammerton, R.E. Cline Jr., The sonochemical hot spot, J. Am. Chem. Soc. 108 (1986) 5641–5642, https://doi.org/10.1021/ja00278a055.
[14] F.R. Young, Sonoluminescence, CRC Press, Boca Raton (2004), https://doi.org/10.1201/9780203491959.
[15] B. Gompf, R. Gunther, G. Nick, R. Pecha, W. Eisenmenger, Resolving sonoluminescence pulse width with time-correlated single photon counting, Phys. Rev. Lett. 79 (1997) 1405–1408, https://doi.org/10.1103/PhysRevLett.79.1405.
[16] D.F. Flannigan, K.S. Suslick, Plasma formation and temperature measurement during single-bubble cavitation, Nature 434 (2005) 52–55, https://doi.org/10.1038/nature03361.
[17] N.C. Eddingsaas, K.S. Suslick, Evidence for a plasma core during multibubble sonoluminescence in sulfuric acid, J. Am. Chem. 129 (2007) 3838–3839, https://doi.org/10.1021/ja070192z.
[18] K.S. Suslick, N.C. Eddingsaas, D.J. Flannigan, S.D. Hopkins, H. Xu, Extreme conditions during multibubble cavitation: sonoluminescence as a spectroscopic probe, Ultrason. Sonochem. 18 (2011) 842–846, https://doi.org/10.1016/j.ultsonch.2010.12.012.
[19] V. Misik, N. Miyoshi, P. Riesz, EPR spin-trapping study of the sonolysis of H_2O/D_2O mixtures: probing the temperatures of cavitation regions, J. Phys. Chem. 99 (1995) 3605–3611, https://doi.org/10.1021/j100011a030.
[20] Y.T. Didenko, W.B. McNamara III, K.S. Suslick, Hot Spot Conditions during Cavitation in Water, J. Am. Chem. Soc. 121 (1999) 5817–5818, https://doi.org/10.1021/ja9844635.
[21] S. Merouani, O. Hamdaoui, Y. Rezgui, M. Guemini, Theoretical estimation of the temperature and pressure within collapsing acoustical bubbles, Ultrason. Sonochem. 12 (2005) 325–329, https://doi.org/10.1016/j.ultsonch.2013.05.008.
[22] E.J. Hart, C.-H. Fischer, A. Henglein, Sonolysis of hydrocarbons in aqueous solution, Radiat. Phys. Chem. 36 (1990) 511–516, https://doi.org/10.1016/1359-0197(90)90198-Q.
[23] A. Tauber, G. Mark, H.-P. Schuchmann, C. von Sonntag, Sonolysis of tert-butyl alcohol in aqueous solution, J. Chem. Soc., Perkin Trans. 2 (2) (1999) 1129–1135, https://doi.org/10.1039/A901085H.
[24] J. Rae, M. Ashokkumar, O. Eulaerts, C. von Sonntag, J. Reisse, F. Grieser, Estimation of ultrasound induced cavitation bubble temperatures in aqueous solutions, Ultrason. Sonochem. 12 (2005) 325–329, https://doi.org/10.1016/j.ultsonch.2004.06.007.
[25] E. Ciawi, J. Rae, M. Ashokkumar, F. Grieser, Determination of temperatures within acoustically generated bubbles in aqueous solutions at different ultrasound frequencies, J. Phys. Chem. B 110 (2006) 13656–13660, https://doi.org/10.1021/jp061441t.
[26] S. Stoll, A. Schweiger, EasySpin, a comprehensive software package for spectral simulation and analysis in EPR, J. Magn. Reson. 178 (2006) 42–55, https://doi.org/10.1016/j.jmr.2005.08.013.
[27] Pub Chem, National Center for Biotechnology Information, National Library of Medicine, 2022 https://pubchem.ncbi.nlm.nih.gov/.
[28] C.K. Holland, R.E. Apfel, An improved theory for the prediction of microcavitation thresholds, IEEE Trans. Ultrason. Ferroelectr. Freq. Control 36 (1989) 204–208, https://doi.org/10.1109/58.19152.
[29] E. Ciawi, M. Ashokkumar, F. Grieser, Limitations of the methyl radical recombination method for acoustic cavitation bubble temperature measurements in aqueous solutions, J. Phys. Chem. B 110 (2006) 9779–9781, https://doi.org/10.1021/jp0618734.
[30] E.A. Neppiras, Acoustic cavitation, Phys. Rep. 61 (1980) 159–251, https://doi.org/10.1016/0370-1573(80)90115-5.
[31] P. Jarman, Measurements of sonoluminescence from pure liquids and some aqueous solutions, Proc. Phys. Soc. 73 (1959) 628–640, https://doi.org/10.1088/0370-1328/73/4/312.
[32] D. Wang, P. Wang, S. Wang, Y.-H. Chen, H. Zhang, A. Lei, Direct electrochemical oxidation of alcohols with hydrogen evolution in continuous-flow reactor, Nat. Commn. 10 (2019) 2796, https://doi.org/10.1038/s41467-019-10928-0.
[33] B.C. Moon, B. Bayarkhii, K.A.I. Zhang, D.K. Lee, J. Byun, Solar-driven H_2O_2 production via cooperative auto- and photocatalytic oxidation in fine-tuned reaction media, Energy Environ. Sci. 15 (2022) 5082–5092, https://doi.org/10.1039/D2EE02504C.
[34] G.R. Buettner, Spin trapping: ESR parameters of spin adducts, Free radical Biol. Med. 3 (1987) 259–303, https://doi.org/10.1016/s0891-5849(87)80033-3.
[35] K. Makino, M. Morssoba, P. Riesz, Chemical effects of ultrasound on aqueous solutions. Evidence for hydroxyl and hydrogen free radicals (·OH and ·H) by spin trapping, J. Am. Chem. Soc. 104 (1982) 3537–3539, https://doi.org/10.1021/ja00376a064.